Parabolic Trough Collector Defocusing Analysis: two control stages vs four control stages

A. J. Sánchez[a,*], A. J. Gallego[a], J. M. Escaño[a], E. F. Camacho[a]

[a]*Departamento de Ingeniería de Sistemas y Automática, Universidad de Sevilla, Camino de los Descubrimientos s/n, 41092 Sevilla, Spain*

Abstract

In solar thermal plants, as in any industrial process, it is important to maintain good control of the system and, more importantly, to have a good security system to avoid exceeding the safety limits of the components and avoid their degradation. In the case of solar thermal plants, one of the main components is the Heat Transfer Fluid (HTF), which must be kept below a maximum temperature. Although the temperature of the fluid, in general, will be controlled by modifying the flow-rate, when the plant is saturated HTF temperature is kept under limits by defocusing of the collectors.

In this paper, an analysis of the control of the defocus control applied to the different collectors is presented. A Model Predictive Control technique will be applied to control the temperature by defocusing two and four collectors in different situations. It is shown how controlling the temperature by defocusing only two collectors is not sufficient in all situations and that controlling by defocusing the four collectors solves this problem in addition to maintaining the defocus actions in areas with high control authority.

Keywords: Solar Energy, Collector defocus analysis, Model Predictive Control, Electric power limitation

1. Introduction

The sun floods the earth with huge amounts of energy every day. An energy that will only run out on the day of the star's death. Only a small part of this energy is absorbed by the earth and is the base of all living beings on this planet (in one way or another), the rest of the energy returns to space. Due to the current great interest in the reduction of CO_2 levels caused, among others, by the emissions generated by conventional power plants (fossil) (Romero and González-Aguilar, 2014; Blanco and Miller, 2017), research and development in relation to renewable energy sources is being promoted more and more, being solar the most abundant and promising of all.

This paper focuses in Concentrating Solar Power (CSP) plants with Parabolic Trough Collectors (PTC). Currently, electricity generation by thermal solar plants is a fact with almost 100 commercial solar plants producing in 2017 (Pitz-Paal, 2018). It is important to highlight one of the best characteristics that solar thermal technology plants have: thermal energy storage (Liu et al., 2016; Alva et al., 2017; Pelay et al., 2017; Sarbu and Sebarchievici, 2018). Although molten salts are generally used in storage tanks (Roca et al., 2016; Peiró et al., 2018), energy storage using steam is also possible (Prieto et al., 2018). However, the use of molten salts seems to be the most recommended when a large storage capacity is needed (González-Roubaud et al., 2017), as occurs in commercial solar plants. Currently, there are parabolic-trough solar plants operating in Spain (Majadas I (50 MW) (NREL Majadas, 2020)), USA (Solana 280 MW (NREL Solana, 2020)), and South Africa (KAXU 100 MW (NREL KAXU, 2020) among others. There is currently a 600 MW project (3 CSP plants, 200 MW each), with a total solar field of 28 square kilometers and 15 hours of thermal storage, under construction by Abengoa Solar in Dubai, United Arab Emirates, launched by Dubai Electricity & Water Authority (DEWA) (NREL DEWA, 2020; Helioscsp.com News, 2020).

PTC CSPs generally operate in a nominal high temperature zone. One of the main objectives in this type of plants is to maintain the outlet temperature around a designated value or nominal set-point. However, this is not the only objective pursued in research. Significant efforts are also being made in research related to production optimization, cost reduction and improvements of thermal storage methods to name just a few. In Camacho and Gallego (2013) an optimization of a solar plant is presented by applying a hierarchical structure of 3 layers to calculate the optimal solar field temperature to increase the plant performance according to environmental conditions. In Khoukhi et al. (2015), authors presented nonlinear continuous-time Generalized Predictive Control (GPC) of solar plants. A control for solar field temperature based on a Dynamic Matrix Control (DMC) is proposed in Lima

*Corresponding author

Email addresses: asanchezdelpozo@us.es (A. J. Sánchez), gallegolen@hotmail.com (A. J. Gallego), jescano@us.es (J. M. Escaño), efcamacho@us.es (E. F. Camacho)

et al. (2016) where a filter is included for the prediction of the error, improving the properties of disturbance rejection and robustness of the DMC. A model-based predictive control (MPC) strategy is presented in Vasallo and Bravo (2016) which is used in conjunction with short-term direct normal irradiance forecast to perform optimal scheduling in CSP plants. In Gallego et al. (2016) a mathematical model of the new TCP-100 solar field of the Plataforma Solar de Almería is developed. In Cojocaru et al. (2019), the authors propose to include a term that penalizes the generation variation (cycling) to reduce it without losing benefit in the power cycle increasing the useful life of the cycle. In Sánchez et al. (2019b), a nonlinear optimization analysis and strategy is presented along with clustering to calculate the necessary control actions on the loops inlet valves to obtain a thermal balance of the solar field reducing the need for unnecessary defocus actions and maintaining loops at similar temperatures. Aguilar et al. (2019) discusses the use of super-critical carbon dioxide (sCO2) to replace current HTFs in PT CSP plants in order to increase the solar-to-electric efficiency of the plant.

A very important aspect is the safety of the plant components, including the heat transfer fluid. It is important never to exceed the temperature limit of the HTF provided by the manufacturer. In the case of diphenyl oxide (DPO) and biphenyl mixture fluids such as Therminol VP1 or similar, this temperature limit is around 400 °C. Defocus control is primarily focused on controlling the fourth (last) collector outlet temperature. However, the defocus control should only have to be applied in flow saturation situations.

However, applying defocus over the fourth collector is often not enough to keep the temperature of the loops within the established safety limits. This will generally occur during the summer season on days of high radiation and in cases of power limitation. Defocus control of the other collectors is needed to keep the temperature below the safety limit.

In this paper the defocus control on the different collectors is analyzed. Applying the defocus on the last two collectors can, in certain situations, meet the objective and keep the outlet temperature of the loops below the safety limit. However, this may be accomplished at the cost of making the defocus controller work with high defocusing angles in a zone of low control authority. The behavior of defocus controllers on different collectors and with different temperature set-points will be simulated and analyzed. It will be shown that applying the defocus control to four collectors provides a better control, solving problems of excess temperature, although at the cost of a greater number of actions when using more control levels in the collectors.

The paper is organized as follows: Section 2 section briefly describes the work prior to this work. In section 3 the model of the 50 MW plant and mathematical models are presented. Section 4 describes the GS-GPCs controller for defocus and power control. Section 5 presents the parameters and simulations of the controllers when applied to collectors 3 and 4. The simulation results and parameters when applying the GS-GPC on the four collectors are shown in section 6. In Section 7 the numerical results of the simulations are presented and a discussion is made regarding the advantages and disadvantages of both strategies. Finally, the papers draws to and end in Section 8 with some conclusions and future work.

2. Related work

Model-based predictive control strategies were presented to control the outlet temperature of the third and fourth collectors of 50 MW solar plants by defocusing in Sánchez et al. (2018, 2019a). It was shown that defocusing the fourth collector was not sufficient, in all situations, to keep the oil temperature below the safety limit. A controller for defocusing the third collector was added to help the fourth and prevent the defocus angle from reaching the control limit. However, in these works, the main purpose was to design and test predictive controllers for defocusing. In fact, the proposed controllers provided good results in tracking the temperature reference for both collectors, keeping the oil temperature below the limits during transients, and under given plant circumstances. However, it is important to emphasize that the level at which the collectors have to be defocused will largely depend on the radiation level, plant flow rate, collector efficiency, plant operating point and possible power limitations. Therefore, it is highly likely that the third and fourth defocus controllers will not be sufficient in all circumstances in order to properly track the loop outlet temperature and avoid the safety limit. In the next sections, an analysis will be presented in various circumstances, presenting the need and convenience of applying the defocus control in the four collectors of the loops of a solar plant.

Since the main objective of the paper is to perform a defocus analysis, a GS-GPC, (Sánchez et al., 2018), will be applied to each of the 4 collectors.

3. 50 MW solar plant model

This section describes the 50 MW plant used, (Sánchez et al., 2018, 2019b). Two mathematical models, a distributed parameter model and a concentrated parameter model, are used for simulation purposes and controller design.

3.1. Parabolic trough field

The solar field of the plant to be simulated occupies around 110 hectares, with 90 loops of 4 collectors each. Each loop is 600 meters long (NREL Guzmán, 2020; NREL Helios, 2020; NREL Solaben, 2020). The main components of a parabolic trough solar plant are the collector, the number of loops, the receiver tube, the HTF and the power cycle.

The HTF used is *Therminol VP1*, widely used for this type of solar application. This fluid begins to degrade from 400 °C. HTF parameters, such as specific heat capacity (C_f) and fluid density (ρ_f), are temperature dependent and can be obtained through equations (1) and (2). All the parameters approximations can be found in Therminol VP1 HTF (2020). The collector used in this plant model is the *EuroTrough ET150*, with similar characteristics to those used in 50 MW commercial plants. The parameters of this collector are shown in Table 1 (Geyer et al., 2002; Kearney, 2007; System Advisor Model (SAM). NREL, 2018). The reflectivity and collector form factor values are assumed to be 0.92 and 0.96 respectively. For the receiver tube, the *Schott PTR70*, very common in commercial plants, is used. The tube is made of steel-type DIN 1.4541 or similar, external diameter of 70mmm and internal diameter of 66mm (Burkholder et al., 2007; SCHOTT Solar CSP GmbH, 2020). The tube efficiency has been assumed to be 0.9.

Table 1
EuroTrough ET150 parameters.

Description	Value	Unit
Focal length	1.71	m
Aperture width	5.77	m
Aperture area	817.5	m^2
Number of Modules per Drive	12	*Unitless*
Length per Solar Collector Assembly (SCA)	148.5	m
SCAs per loop	4	*Unitless*
Heat Collection Element (HCE) Type	*Evacuated tube*	*Unitless*

$$\rho_f = -0.90797 \cdot T + 0.00078116 \cdot T^2 - 2.367 \times 10^{-6} \cdot T^3 + 1083.25 \tag{1}$$

$$C_f = 4.5904 \times 10^{-8} \cdot T^4 - 3.1536 \times 10^{-5} \cdot T^3 + 0.006498 \cdot T^2 + 2.3458 \cdot T + 1500.8 \tag{2}$$

In general, 50 MW commercial plants operate at nominal with 393 °C at the output of the solar field and a return temperature of 293 °C, therefore, the thermal jump is 90-100 °C. Assuming only the losses produced by the parasitic effects (0.9) and the rankine cycle (0.381) (Andasol 1, 2018; NREL Extresol, 2020; System Advisor Model (SAM). NREL, 2018), an approximation of the flow necessary to produce 50 MW (3000 m^3/h approx.) can be obtained using the equation 3, (Sánchez et al., 2019b).

$$Q = \frac{P \cdot 10^6}{\Delta T \cdot C_f \cdot \mu_{rankine} \cdot \mu_{parasitic}} \tag{3}$$

3.2. Distributed parameter model

The distributed solar field dynamics can be described by a partial differential equations (PDE) system shown in equation 4. The system energy balance is described in this set of PDEs (Carmona, 1985; Camacho et al., 1997):

$$\rho_m C_m A_m \frac{\partial T_m}{\partial t} = I K_{opt} n_o G - H_l G (T_m - T_a) - L H_t (T_m - T_f) \tag{4a}$$

$$\rho_f C_f A_f \frac{\partial T_f}{\partial t} + \rho_f C_f q \frac{\partial T_f}{\partial x} = L H_t (T_m - T_f) \tag{4b}$$

Subindexes f and m are used referring to the fluid and metal. Geometric efficiency depends on declination, day of the year, local latitude, collector parameters, solar hour and hourly angle. Coefficients and parameters H_l, specific heat C and density ρ depends on the temperature of the fluid. Coefficient H_t depends on fluid temperature and HTF flow-rate (Camacho et al., 1997). An approximation for H_l can be obtained from Burkholder et al. (2007), Lüpfert et al. (2008). To obtain H_t value, equations (5) are used, where the dependency of the flow-rate can be observed.

$$Re = Q \cdot D / (\nu \cdot A) \tag{5a}$$

$$Pr = C_f \cdot \mu / k \tag{5b}$$

$$Nu = 0.025 \cdot (Re^{0.79}) \cdot (Pr^{0.42}) \cdot phi \tag{5c}$$

$$H_t = Nu \cdot k / D \tag{5d}$$

3.3. Concentrated parameter model

The concentrated parameter model (CPM) is a simplification of the spatially distributed solar field (Camacho et al., 2007, Gallego et al., 2019). This simplification provides an overall description of the solar field in terms of the fluid internal energy variation by equation 6.

$$C_{loop} \frac{dT_{out}}{dt} = K_{opt} n_o S I - q C_f \rho_f (T_{out} - T_{in}) - H_l S (T_{mean} - T_a) \tag{6}$$

where q is the HTF flow-rate, T_{out} and T_{in} are the outlet and inlet oil temperatures of the model, T_{mean} is the average value between outlet and inlet temperatures and T_a is the ambient temperature. C_{loop} is the thermal capacity, approximated by 3.8×10^6 J/°C, K_{opt} is the optical efficiency (mirror reflectivity, tube absorptance, and interception factor), I is the direct solar irradiance and S is the reflective surface of the loop, 3427 m^2.

4. Generalized predictive control

The GPC algorithm is based on the following single-input single-output model (Camacho and Bordons, 2007):

$$A(z^{-1}) y_k = z^{-d} B(z^{-1}) u_{k-1} + \frac{C(z^{-1})}{\Delta} e_k \tag{7}$$

where u_k and y_k are the control and output sequences of the plant, e_k is a zero mean white noise term and Δ is the integrator operator. A, B and C are polynomials in the backward shift operator z^{-1}:

$$A(z^{-1}) = 1 + a_1 z^{-1} + ... + a_{na} z^{-na}$$
$$B(z^{-1}) = b_0 + b_1 z^{-1} + ... + b_{nb} z^{-nb}$$
$$C(z^{-1}) = 1 + c_1 z^{-1} + ... + c_{nc} z^{-nc}$$

where d is the dead time of the system and Δ is the operator $1 - z^{-1}$. This model is known as a Controller Auto-Regressive Integrated Moving-Average (CARIMA) model. Consider a multistage cost function of the form:

$$J(N_1, N_2, N_u) = \sum_{j=N_1}^{N_2} \delta(j)[\hat{y}(k+j|k) - w(k+j)]^2 + \sum_{j=1}^{N_u} \lambda(j)[\Delta u(k+j-1)]^2 \quad (8)$$

where $\hat{y}(k+j|k)$ is an optimum j step ahead prediction of the system output, N_1 and N_2 are the minimum and maximum costing horizons, N_u is the control horizon, $\delta(j)$ and $\lambda(j)$ are weighting sequences and $w(k+j)$ is the future reference trajectory. The aim of GPC is to minimise $J(N_1, N_2, N_u)$ in order to compute a future sequence of control actions $u(k), u(k+1), ...$ that drives the future plant output $y(k+j)$ close towards $w(k+j)$.

Lets consider the following Diophantine equation:

$$1 = E_j(z^{-1})\tilde{A}(z^{-1}) + z^{-j} F_j(z^{-1}) \quad (9)$$

where $\tilde{A}(z^{-1}) = \Delta A(z^{-1})$. The polynomials E_j and F_j are uniquely defined with degrees $j-1$ and n_a respectively.

By operating with the Diophantine equation (9) and the CARIMA plant model (7) the following expression for the system output can be obtained:

$$\mathbf{y} = \mathbf{G}\mathbf{u} + F(z^{-1})y(t) + \mathbf{G}'(z^{-1})\Delta u(t-1) \quad (10)$$

The Eq. (10) can be compacted into two parts, (11), since the last two terms depend only on the past:

$$\mathbf{y} = \mathbf{G}\mathbf{u} + \mathbf{f} \quad (11)$$

where f is known as the free response of the system. Finally the expression (8) can be written as:

$$J = (\mathbf{G}\mathbf{u} + \mathbf{f} - \mathbf{w})^T(\mathbf{G}\mathbf{u} + \mathbf{f} - \mathbf{w}) + \lambda \mathbf{u}^T\mathbf{u} \quad (12)$$

Hence given a CARIMA plant model and suitable cost function, the minimum of the cost function can be obtained by setting the gradient of $\mathbf{J}$ equal to zero and solving the control sequence $\Delta\mathbf{u}$ by the following equation (Camacho and Bordons, 2007):

$$\Delta\mathbf{u} = (\mathbf{G}\mathbf{G}^T + \lambda\mathbf{I})^{-1}\mathbf{G}^T(\mathbf{w} - \mathbf{f}) \quad (13)$$

where matrix $\mathbf{G}$ contains the step response coefficients of the forced response model (Camacho et al., 2012), $\mathbf{I}$ is the eye matrix, $\mathbf{f}$ is the free response of the plant, $\mathbf{w}$ is the future reference trajectory vector and λ is the control weighting vector (Camacho and Bordons, 2007).

4.1. Defocus GS-GPC Control

For the control of the temperature by defocus collectors, a GPC control with a Gain Scheduling (GS) will be used. In order to design this controller it is necessary to consider the defocus curve. This curve is presented in Fig. 1 (Goswami et al., 2000) and it can be seen how it is not only nonlinear but also has 3 clearly identifiable zones. Two areas where it is necessary to send important actions to the collector in order to decrease or increase the collector's efficiency level (0-1 and 4-5 degrees). Notice that above 3 degrees of defocus the efficiency goes below 20 %. The curve presents a third zone, around 2.5 degrees of defocus, where a high slope can be observed, that is, small control actions will cause large changes in the efficiency of the collector.

Using the GS makes it possible to approximately include the nonlinear characteristic of this curve in the GPC controller. For this, several linear models are obtained at different defocus and flow-rate operating points. Similar to (Sánchez et al., 2018), the GS is designed at nine different points of defocus angle (0.5, 1, 1.5, 2, 2.5, 3, 3.5, 4 and 4.5 degrees). In addition, in order to cover the entire possible operating range of the plant, the nine linear models will be obtained at different flow operation points (1494, 1908, 2322 and 2736 m^3/h).

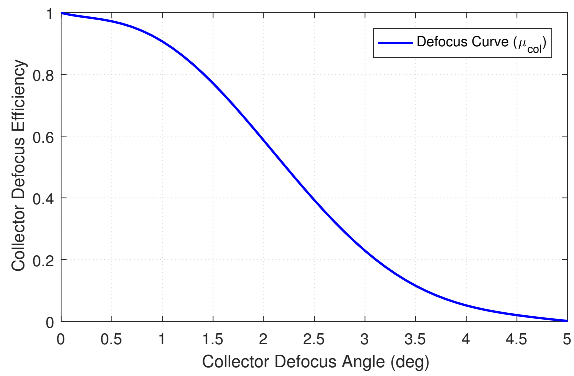

Figure 1 Collector efficiency-defocus angle curve.

4.2. Power limitation GPC control

Solar plants may receive orders commanded by the Transmission System Operator (TSO) to limit its generated power, mainly due to the saturation of the grid. In order to reduce the power, the flow must be reduced and the HTF temperature may rise to undesirable values if not appropriate measures are taken.

In order to control the power generated a GS-GPC will be used which uses the HTF flow as manipulated variable.

As done with the defocus GPC, different linear models can be obtained to capture the dynamics of the plant that strongly depends on the flow-rate (Schenk et al., 2015; Montañés et al., 2018). Linear models at 3 different flow points are used to capture the non-linearity of the plant, approximately, and include it in the GPC: 167.06, 334.1 and 501.16 kg/s (855, 1710 and 2565 m^3/h). Upon receiving a power limitation, the plant will have a known time, specified by the TSO, to reach the power set-point. One of the advantages of using MPC strategies is the sliding horizon. Since the time at which the power set-point has to be reached is known, set-point ramps can be created for the controller at each control instant and thus achieve better tracking of the trajectory during the power drop until reaching the power set-point, (Sánchez et al., 2018).

5. Defocus control: 3rd and 4th collectors

In this section, various results will be presented when applying the control strategy in the third and fourth collectors of the loops. The temperature set-points used in previous works will be used for collector 3 and 4 (Sánchez et al., 2018). The temperature of the fourth collector will be 393 °C if the plant is in power limitation and close to or in flow saturation, otherwise the temperature will be somewhat higher, 395 °C, to avoid coupling between the defocus controllers and the global temperature flow-rate controller. The temperature of the third collector was chosen taking into account the defocus curve (Sánchez et al., 2018). The defocus curve is non-linear with a steep slope around 2.5 degrees. Above 3 degrees, the efficiency of the collector is observed to be very close to zero. Working above this angle implies very little control authority, i.e., big increments in the control actions implies small changes in the efficiency. Therefore, a temperature of 385 °C was chosen by simulation for the third collector. This temperature caused the third collector to defocus out at high temperature, keeping the action of the fourth collector below 3 degrees of defocusing.

5.1. Control sample time and parameters

In commercial plants, the defocusing strategy is carried out using partial and total defocusing, which can cause significant fluctuations in the loops outlet temperatures. The fact of proposing and applying MPC strategies such as the GS-GPC does not imply that this safety strategy is eliminated, although modifying the operating temperature for it. In previous works, (Sánchez et al., 2018, 2019a), a sampling time of 30 s was selected for the defocus GS-GPC controller. This time was found to be sufficient, in general, to properly tract the temperature set-point. It was observed that the fluid temperature did not, under any circumstances, exceed the limit temperature. In very extreme cases, where the temperature could exceed this limit, the partial and/or total defocus safety strategy could perfectly coexist with the proposed GS-GPC strategy. However, to try to avoid activating this security strategy, the sampling time of the GPC controllers that are applied to each of the loops has been modified.

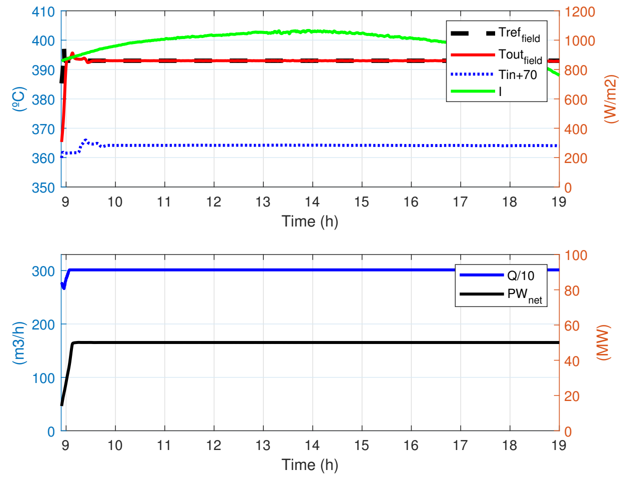

Figure 2 High radiation day. 4th and 3rd collectors GS-GPCs. Field and inlet temperatures, flow and power results.

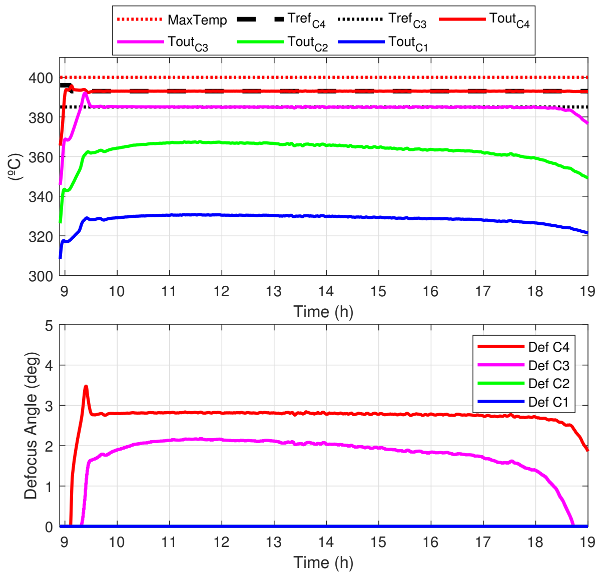

Figure 3 High radiation day. 4th and 3rd collectors GS-GPCs. Collectors temperatures and defocus actions.

It must be taken into account that since a control for reference tracking is being applied, the sampling times must be in line with the dynamics of the process. That is, very long sampling times should not be chosen since then the GS-GPC would not work properly for tracking the temperature reference applied to each of the collectors. Therefore, the following sampling times have been applied for each of the collector controllers:

1. Sample time GS-GPC Collector 3: 30s

2. Sample time GS-GPC Collector 4: 5s

The sampling time of 30 seconds in collector 3 has been maintained since it has already given a good result in previous works. However, the fourth collector sampling time has been reduced to 5 seconds since it is the one that will mainly prevent the temperature from exceeding the safety limit in very extreme cases, thus avoiding the possible use of the final security strategy.

Regarding the weights of the control actions, although correct tracking of the different temperatures set-points is intended, it is also important to avoid activating high-frequency dynamics and causing oscillations in the actions and on the temperatures. A weight $\lambda_{C4} = 2000$ has been chosen for the fourth collector. Since the controller now sends control actions every 5 seconds, it can also be more sensitive to activating the commented modes. For the third collector, a $\lambda_{C3} = 1000$ has been chosen, providing temperature tracking and smooth control actions. These values have also been chosen in relation to the following subsection which talks about the precision in the performance of the defocus actuators. As for the control and prediction horizons, for the GS-GPC of the third collector, which is controlled every 30 seconds, the same horizons are used as in (Sánchez et al., 2018), that is, N2 = 12 and Nu = 6. Regarding the GS-GPC of the fourth collector, since it has been sampled at 5 seconds, the horizons have been increased and the chosen values for this work are N2 = 90 and Nu = 50.

Figs. 2 and 3 show the results of applying GS-GPC controllers to the third and fourth collector on a day of high Direct Normal Irradiance (DNI). It can be seen how the control signals are smooth, producing a good tracking of the reference temperatures for collectors 3 and 4. The control actions of the third collector are centered on approximately 2 degrees while the fourth is a little below 3 degrees, as intended when selecting 385 °C as the reference temperature for the third collector.

5.2. Minimum defocus angle constraint

Although a good behavior of the GS-GPC controller for defocusing is observed, it should be noted that in these simulations, the control signal that is applied to the collector does not undergo any modification. In reality, due to the actuators physical limitations, there will be a minimum angle increment on the collector. For this work, a precision of the collector increments of 0.1 degrees is assumed based on the actuators manufactured by HELAC Corp. (model L30-380) (Heney, 2020).

Obviously, having a more unprecise control signal will cause loss of precision in the set-point tracking. From now on, all the simulations will be done using the 0.1 degrees in the precision of the increments and it will shown that no different control signals will be sent to the actuator in each iteration of the controllers. Moreover, despite the precision in the control, it will be checked that the temperature tracking will still have a good performance.

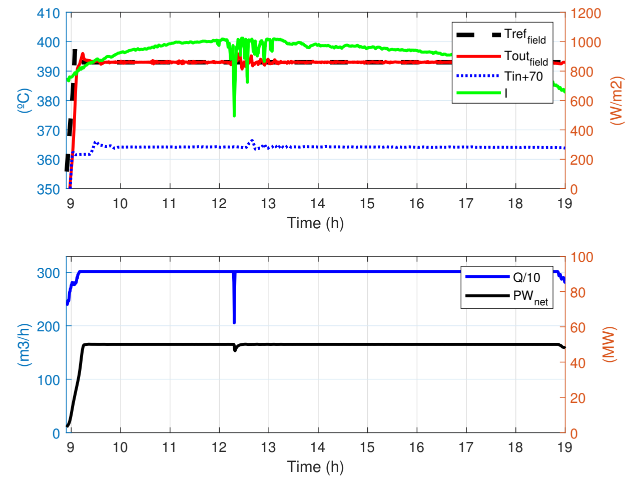

Figure 4 High radiation day with transients. 4th and 3rd collectors GS-GPCs (precision 0.1 degrees). Field and inlet temperatures, flow and power results.

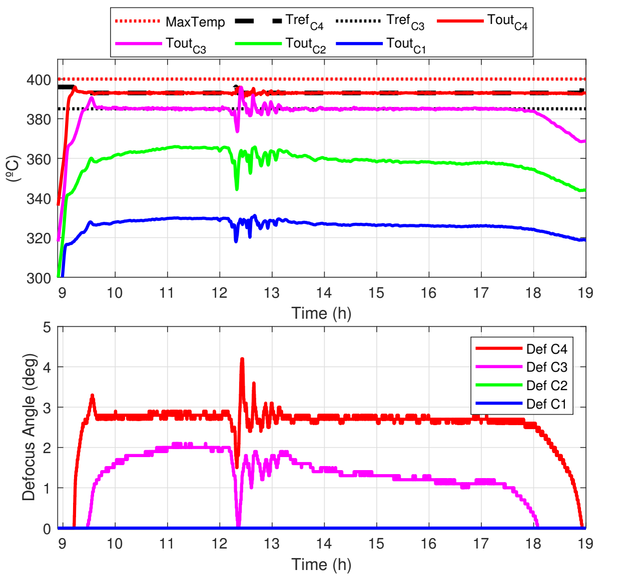

Figure 5 High radiation day with transients. 4th and 3rd collectors GS-GPCs (precision 0.1 degrees). Collectors temperatures and defocus actions.

Regarding the behavior of the strategy on transient days when the radiation is high, simulation results are presented in Figs. 4 and 5. It can be seen that both collectors respond adequately to transients to avoid loss of temperature. Due to the high radiation and the abrupt transient, the defocus controllers have to act decisively to avoid the strong loss of temperature.

5.3. Inlet temperature disturbance rejection

In this section we test how the defocus controller is able to cope with significant disturbance in the inlet temperature. It is important to emphasize that the GS-GPC controllers do not use the inlet temperature of the loop, nor the inlet temperature of the collectors, therefore the behavior of the controller when faced with such disturbances should be analyzed.

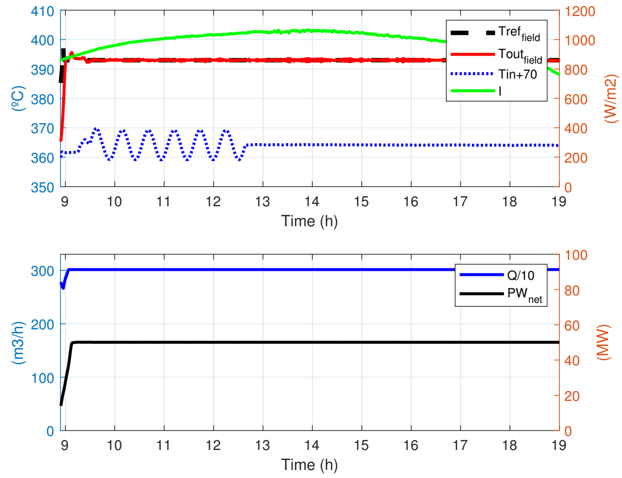

Figure 6 Inlet temperature disturbance. 4th and 3rd collectors GS-GPCs (precision 0.1 degrees). Field and inlet temperatures, flow and power results.

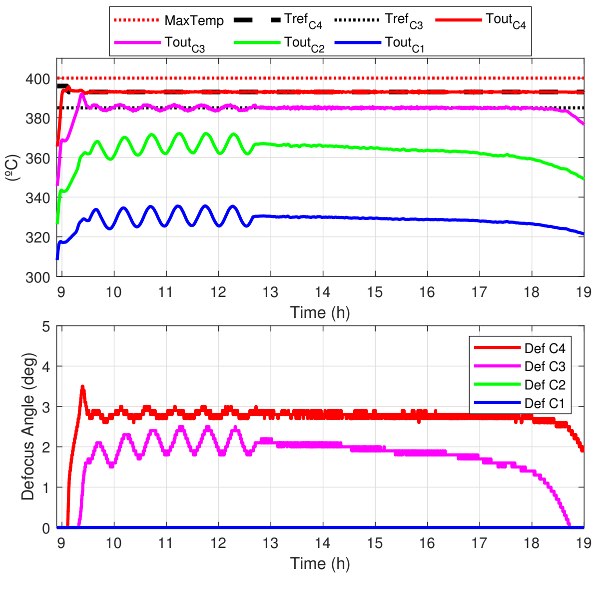

Figure 7 Inlet temperature disturbance. 4th and 3rd collectors GS-GPCs (precision 0.1 degrees). Collectors temperatures and defocus actions.

In the simulation presented in Figs. 6 and 7, a sine wave added to the inlet loop temperature of 10 degrees peak to peak has been applied with a period of about 30 minutes. This type of disturbance in the input temperature is not common in practice, since for this to happen in reality, the field outlet temperature would also have to be oscillating with a greater amplitude of the oscillation, which would imply a poor control of the field outlet temperature. However, it is important to observe the behavior against strong disturbances.

Since collectors 1 and 2 are free of control (always tracking the sun), the input temperature disturbance is transmitted throw both collectors. It can be seen that the GS-GPCs of the third and fourth collector manage to reject this disturbance. The third collector cannot completely reject the disturbance, having an oscillating follow-up of its reference temperature, although these control actions decrease the amplitude of the disturbance (from 10 °C to 3 °C peak to peak).

The fourth collector is the one that, thanks to the help of the third collector largely rejecting the disturbance, finally achieves its objective and maintains good tracking of the reference temperature. Compared with the result in tracking the outlet temperature of both collectors, it can be seen how the actions in the third collector are more important than in the fourth which can regulate its temperature through smaller control actions due to the help of the third.

5.4. 30 MW Power limitation

To observe the behavior of the GS-GPC controllers applied to the third and fourth collector in cases of significant power limitations on days of very high radiation, a case is simulated where the plant is limited to 30 MW. This case is shown in Figs. 8 and 9.

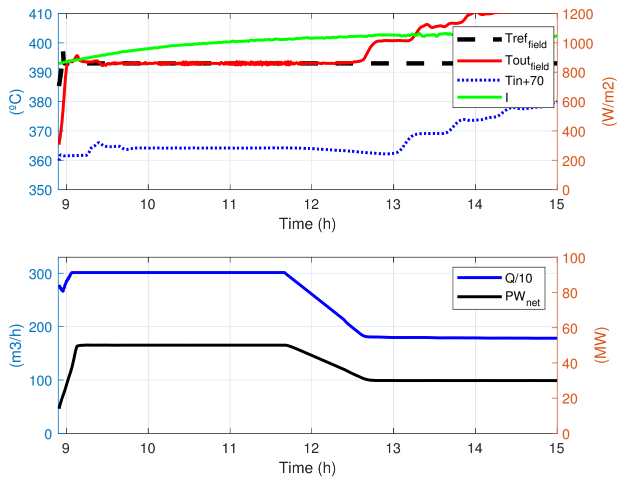

Figure 8 30 MW power limitation scenario. 4th and 3rd collectors GS-GPC (precision 0.1 degrees). Field and inlet temperatures, flow and power results.

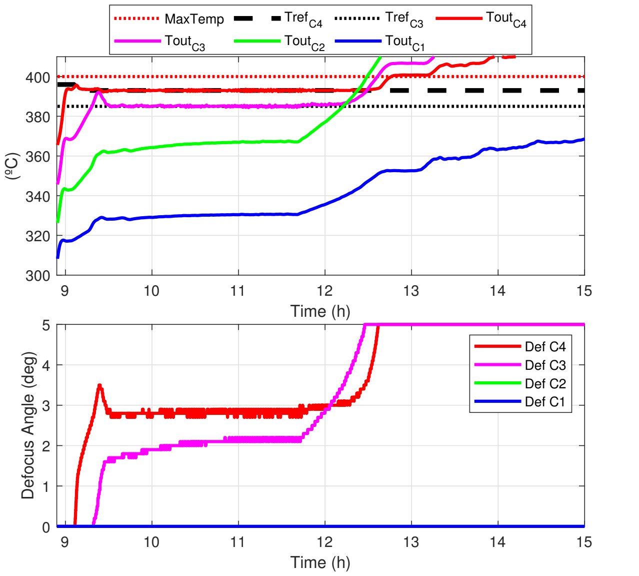

Figure 9 30 MW power limitation scenario. 4th and 3rd collectors GS-GPC (precision 0.1 degrees). Collectors temperatures and defocus actions..

As previously mentioned, it can be seen in Figs 8 and 9, how both controllers work correctly until the power limitation arrives. The power controller begins to decrease the flow to reach, in the stipulated time by the TSO, the 30 MW set-point. As the flow rate decreases, the defocus angle applied by the third and fourth GS-GPCs increases to compensate for the lack of flow control over the loop outlet temperature. Reaching the point at which the third collector reaches its saturation (5 degrees - 0 efficiency) first, since it is designed to help the fourth. Secondly, the fourth collector ends up also reaching saturation so that, between the flow dedicated to power control and the lack of control due to defocusing, the temperature becomes uncontrollable and it shoots up exceeding the temperature limit. As discussed, defocusing the third and fourth can be sufficient in most situations, but not all, therefore, more levels of control are required.

6. Using four collectors GPC defocus control

Although it has been observed that the control with the third and fourth collector can keep the outlet temperature within the safety limit even on very high radiation days, it is also observed that the fourth collector is centered approximately around 3 degrees of defocusing. Reviewing Fig. 3, it can be seen that in this area the collector efficiency is 0.2 approx., while the third collector maintains an approximate value of about 2 degrees, which means a collector efficiency of 0.6. Since the controller is already close to the area where the control capacity is low, it could happen that it was not capable of maintaining good temperature control in the face of certain external events, such as strong transients or more power limitations. In fact, it has been shown in the previous section how the GS-GPC applied in the third and fourth collector are not capable of maintaining the temperature below the limit in a 30 MW power limitation situation.

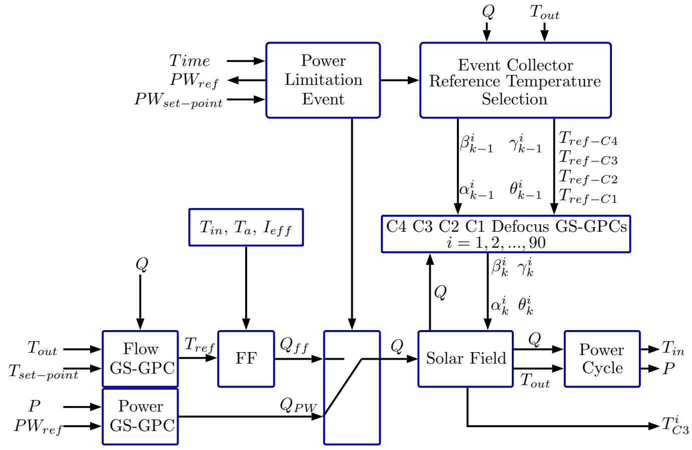

Figure 10 Full control strategy scheme

In fact, it has been shown in the previous section, see Figs. 8 and 9, how the GS-GPC applied in the third and fourth collector are not capable of maintaining the temperature below the limit in a 30 MW power limitation situation. Since loops have four collectors, to prevent the controller from getting too close to the low control authority area, one option is to extend the blur controller to all four collectors. In this case, it would only be necessary to add a GS-GPC in the first and second collectors, which will help to lower the actuation levels of the third and fourth, keeping the control actions in a more appropriate control area. The control scheme is illustrated in Fig. 10.

6.1. Temperature reference and control parameters

By adding the GS-GPC control on collectors 1 and 2, a further stage of aid in temperature control is being included by the defocus control of the fourth collector. In other words, it is no longer necessary for the reference temperature of the third collector to be around 385 °C as in the previous simulations. Furthermore, it is now necessary to select 3 new reference temperatures for the first, second and third collector controllers. Once again the problem of deciding which temperatures to choose arises. The case of the fourth collector is simple since it is directly linked to the nominal working point of the plant. However, in the case of defocusing the other collectors, it may be somewhat complex and/or subjective, given that according to the chosen operating criteria different reference temperatures for defocusing would be obtained.

The criterion chosen in this article to select these temperatures is to try to maintain, as far as possible and according to environmental circumstances, the same level of defocusing in the four collectors. For this, what is done is to divide the thermal jump into four parts (under nominal operating conditions 100 °C, inlet 293 °C, outlet 393 °C approx.). Which gives us a thermal jump per collector of about 25 °C. And to ensure a little more temperature at the exit of the fourth collector, these temperatures are increased by 1 °C and with this the new reference temperatures for the four collectors are obtained:

1. Temperature set-point collector 1: 319 °C
2. Temperature set-point collector 2: 344 °C
3. Temperature set-point collector 3: 369 °C
4. Temperature set-point collector 4: 393/395 °C

A sampling time of 30 s has been chosen for the controllers of the first and second collectors. This is a reasonable time to obtain a good tracking of the temperature set-point. The weights for the control actions chosen for the GS-GPC of the first and second collector are: $\lambda_{C1-C2} = 500$. These weights are chosen so that the first and second collectors are the main chain elements to absorb the disturbances. One of the objectives is to prevent the fourth collector from causing oscillations by activating high frequencies trying to reject all the disturbances. Since these two controllers are also sampled at 30 seconds, the control and prediction horizons are the same as in the case of the third collector, discussed above.

The simulation of the high DNI with transients scenario is carried out taking into account a precision of 0.1 degrees in the control signal. Fig. 11 shows the simulation results. It is observed that despite using 4 GS-GPC controllers in series and applying the precision in the actuation, the controllers show a good performance overall.

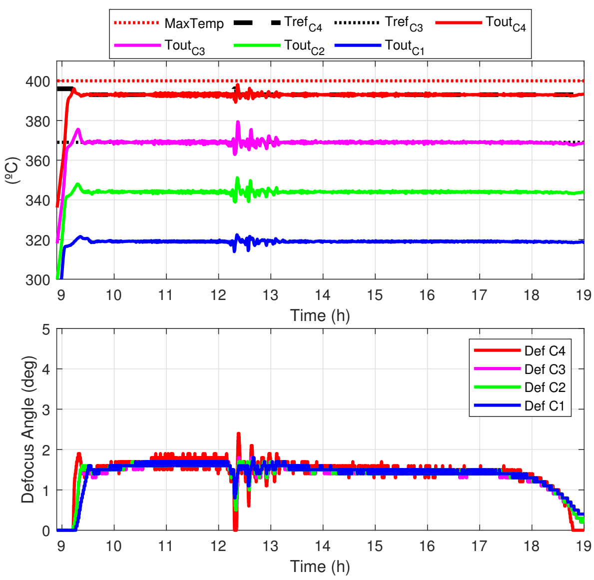

Figure 11 High radiation day with transient. 4th, 3rd, 2nd and 1st collectors GS-GPCs (precision 0.1 degrees). Collectors temperatures and defocus actions.

It can be observed that the radiation disturbance is rejected correctly maintaining the temperature within the safe limit. Despite having a day with very high radiation, the distribution of the control among the four collectors provides a good temperature tracking while maintaining a performance level around 1.7 degrees of defocus per collector (0.7 efficiency approx.), a more comfortable and safe area for the control.

6.2. *Inlet temperature disturbance rejection*

Regarding the rejection of disturbances in the inlet temperature, the sustained oscillation test is carried out. It is to be hoped that by having more control levels, the rejection will be obtained mainly in collectors 1 and 2.

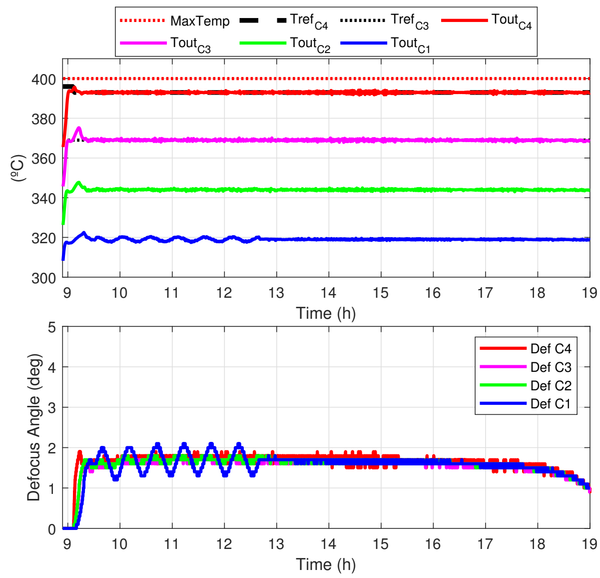

Figure 12 Inlet temperature disturbance. 4th, 3rd, 2nd and 1st collectors GS-GPCs (precision 0.1 degrees). Collectors temperatures and defocus actions.

Fig. 12 presents the results of this simulation. It is clearly seen how the first and second collectors are responsible for rejecting the disturbance that occurs at the inlet. Furthermore, it is the first collector that practically eliminates the disturbance, hence the first GS-GPC control signal has the highest amplitude oscillations. The tracking of the temperature of the fourth collector has a good performance since the disturbance has been absorbed by the first and second collectors.

6.3. *30 MW Power limitation*

In this section, the control of the four collectors is now tested to try to solve the temperature trip problem when there are power limitations on days of high solar radiation.

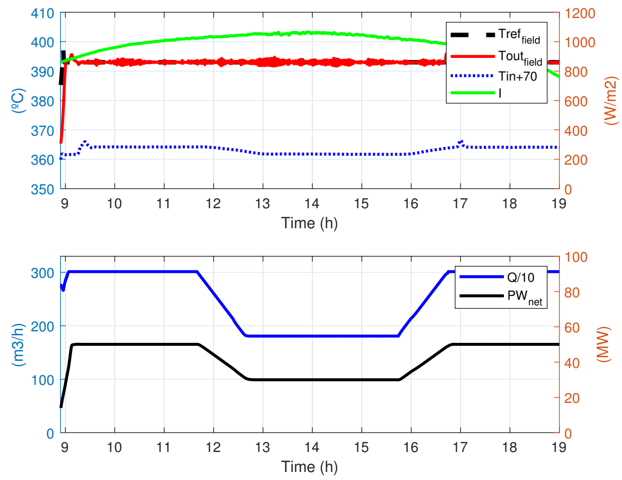

Figure 13 30 MW power limitation scenario. 4th, 3rd, 2nd and 1st collectors GS-GPCs (precision 0.1 degrees). Field and inlet temperatures, flow and power results.

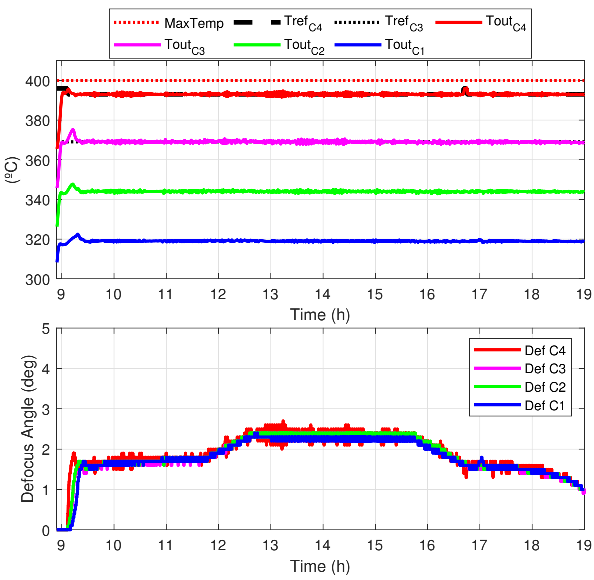

Figure 14 30 MW power limitation scenario. 4th, 3rd, 2nd and 1st collectors GS-GPCs (precision 0.1 degrees). Collectors temperatures and defocus actions.

Figs. 13, 14 and 15 show the results of this simulation. It can be seen how thanks to the four stages of defocus control, not only is it possible to control the field outlet temperature, but it is also observed that a fairly comfortable controller working area is maintained in terms of control capacity, around a maximum of 2.2-2.4 degrees of defocus in the four collectors, see Figs. 13 and 14, during power limitation (0.4-0.5 collector efficiency). Fig. 15 shows a zoom of the area where the flow drop occurs during power limitation. The changes produced in the control actions can be observed.

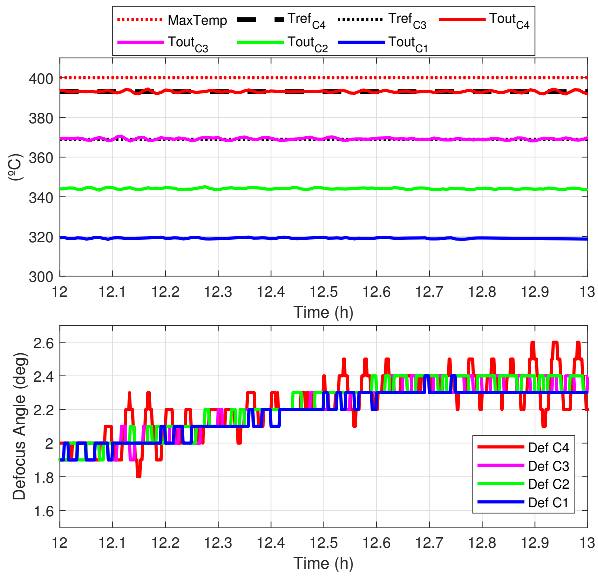

Figure 15 Zoom. 30 MW power limitation scenario. 4th, 3rd, 2nd and 1st collectors GS-GPCs (precision 0.1 degrees). Collectors temperatures and defocus actions.

7. Discussion

Tables 2, 3, 4 and 6 present the results for each of the scenarios and the controllers for two and four collectors. Table 2 illustrates the results when the actuator can move to any angle within the spam of the actuator. The most interesting results in this final discussion are presented in Tables 3, 4, 5 and finally in 6 where the results of the power limitation are presented.

The following indices are included in these tables:

1. Number of Moves: the total number of moves in each collector.
2. Degrees: the number of degrees the collector has moved due to defocus control.
3. Efficiency: average efficiency of the collector in the considered interval.
4. Control Authority: Index that measures the remaining control capacity.

The control authority index has been calculated as shown in Eq. (14). This is, a relation between the efficiency of the collector and the efficiency than can be modified by the collector when it moves 0.5 degrees more. This equation produces the curve shown in 16, which has been normalized, where it can be seen that it gives a maximum value at around 1.43 degrees. It can be observed in the defocus curve, Fig. 1, that this is the point at which the steep slope starts. However, the curve has been modified and the control index has been assumed to be 1 below 1.43 degrees.

$$CI = efficiency \cdot abs(efficiency - eff_{+0.5^{\circ}}) \qquad (14)$$

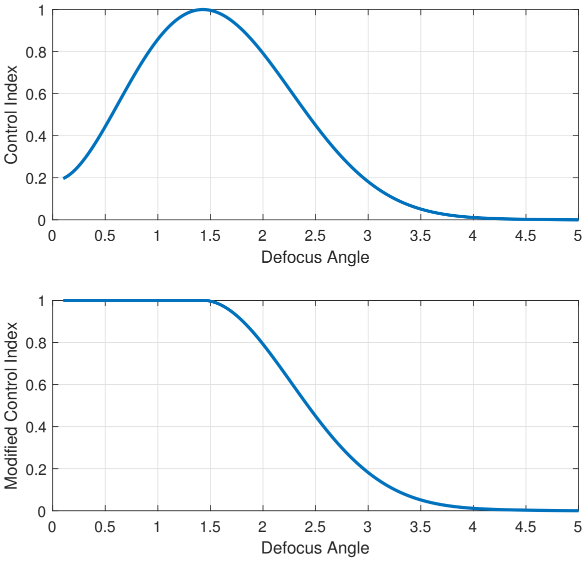

Figure 16 Control Index. Original (top) and Modified (bottom) curves.

In tables 3 and 4 it can be seen that when applying the control in the four collectors, by using two more actuators, more control actions are taken. So it might be thought that the strategy of the four collectors is "worse" than that of the two collectors. However, it can be seen that the efficiency index of the fourth collector is significantly reduced when the controllers are only applied to the third and fourth collectors. Nevertheless, both the third and fourth continue to have control. In contrast, the control index is kept at 1 when using all four collectors control. Furthermore, it is not possible to control with only two collectors in cases of significant power limitations on days with high radiation. By applying the control in a distributed way in the four collectors, it can be seen that it is possible to control and maintain the temperature below the limit in all situations, even in the power limitation where it maintains the 4 collectors in an area where there is still a margin of control in the four collectors.

Table 2
1 Loop results. High Radiation, no precision (9am - 19pm)

Control	3rd, 4th GS-GPC		1st, 2nd, 3rd, 4th GS-GPC			
Index	3rd	4th	1st	2nd	3rd	4th
No. of Moves	1132	7121	1184	1193	1198	7121
Degrees	5.67	7.72	3.77	4.52	4.13	6.58
Efficiency	0.65	0.32	0.77	0.79	0.79	0.73
Control Authority	0.89	0.33	0.99	0.99	0.99	0.98

Table 3
1 Loop results. High Radiation, 0.1º precision (9am - 19pm)

Control	3rd, 4th GS-GPC		1st, 2nd, 3rd, 4th GS-GPC			
Index	3rd	4th	1st	2nd	3rd	4th
No. of Moves	488	1307	407	397	402	1385
Degrees	49	130.7	40.8	39.8	40.3	138.5
Efficiency	0.65	0.32	0.76	0.78	0.77	0.73
Control Authority	0.88	0.33	0.99	0.99	0.99	0.98

Table 4
1 Loop results. High Rad./Transient, 0.1º precision (9am - 19pm)

Control	3rd, 4th GS-GPC		1st, 2nd, 3rd, 4th GS-GPC			
Index	3rd	4th	1st	2nd	3rd	4th
No. of Moves	311	1434	492	489	404	1331
Degrees	32.8	143.4	50.2	51.2	42	134
Efficiency	0.79	0.35	0.80	0.82	0.82	0.77
Control Authority	1	0.3716	1	1	1	0.99

Table 5
1 Loop results. Inlet Temperature Disturbance, 0.1º precision (9am - 19pm)

Control	3rd, 4th GS-GPC		1st, 2nd, 3rd, 4th GS-GPC			
Index	3rd	4th	1st	2nd	3rd	4th
No. of Moves	408	1325	435	483	402	1226
Degrees	41	132.5	43.6	48.4	40.3	122.6
Efficiency	0.65	0.32	0.76	0.78	0.77	0.73
Control Authority	0.88	0.33	0.99	0.99	0.99	0.98

In many situations the temperature of the HTF can be kept within the safety limits by defocusing only two collectors and this may have some advantages. An event-based supervisory system could be implemented in order to change the two controller mode to the four control mode and viceversa. It can also be seen that disturbances at the inlet temperature are better rejected when using more defocus control stages.

Table 6
1 Loop results. 30 MW Power Limit, 0.1º precision (9am - 19pm)

Control	3rd, 4th GS-GPC		1st, 2nd, 3rd, 4th GS-GPC			
Index	3rd	4th	1st	2nd	3rd	4th
No. of Moves	N.A.	N.A.	505	475	394	1347
Degrees	N.A.	N.A.	50.6	47.6	39.5	134.7
Efficiency	0	0	0.67	0.69	0.68	0.64
Control Authority	0	0	0.92	0.93	0.92	0.87

Another important factor is in relation to the temperature set-points of each of the controllers. Since the plant will work in many different circumstances.

8. Conclusion

Operating solar power plant require constantly monitoring the main components of the plant. One of the main component is the HTF fluid. This fluid must not exceed a certain temperature because it degrades and must be replaced at considerable costs. In general, the temperature of the HTF is controlled by manipulating the flow, although, it is not always possible to do as when the HTF flow cannot be increased. In these situations, the defocusing of the collectors keeps the temperature below the safety limit.

In this work, the behavior of model predictive controllers applied to the last two collectors and to all four collectors have been presented and analyzed. The precision of the collector actuators has also been included, which makes the simulations more consistent with the actual behavior of the plant. It has been shown that applying defocus over the third and fourth collector is often not enough to keep the temperature of the loops within the established safety limits. This will generally occur during the summer season on days of high radiation and in cases of power limitation. More levels of defocus control must be added over other collectors in order to keep the temperature below the safety limit. The use of only two collectors has some advantages, such as avoiding the use of the first two actuators by keeping them inactive, although it is not always possible and these controllers reach control areas where they lose authority. The advantage of the control in the four collectors is mainly focused on the fact that this strategy is capable of dealing with all situations in a more comfortable control area. Since it may not always be necessary to use all four collectors, the use of an event-based or even manual (by the operator) system to apply the defocus control to the first two collectors was discussed. An open discussion has also been left regarding the temperature set-points for each of the collectors. The authors intend to continue working on this open topic in future works to find optimal solutions that require less attention from operators to maintain safety in the collectors.

Acknowledgments

The authors would like to acknowledge the European Research Council for funding this work under Advanced Research Grant OCONTSOLAR (789051) and the VI Plan of Research and Transfer of the University of Seville (VI PPIT-US) under the contracts "Contratos de acceso al Sistema Español de Ciencia, Tecnología e Innovación para el desarrollo del programa propio de I+D+i de la Universidad de Sevilla".

References

Aguilar, R., Valenzuela, L., Avila-Marin, A. L., Garcia-Ybarra, P. L., 2019. Simplified heat transfer model for parabolic trough solar collectors using supercritical co2. Energy Conversion and Management 196, 807 – 820.

Alva, G., Liu, L., Huang, X., Fang, G., 2017. Thermal energy storage materials and systems for solar energy applications. Renewable and Sustainable Energy Reviews 68, 693 – 706.

Andasol 1, Sep. 2018.
URL `https://solarpaces.nrel.gov/andasol-1`

Blanco, M., Miller, S., 2017. 1 - introduction to concentrating solar thermal (cst) technologies. In: Blanco, M. J., Santigosa, L. R. (Eds.), Advances in Concentrating Solar Thermal Research and Technology. Woodhead Publishing Series in Energy. Woodhead Publishing, pp. 3 – 25.

Burkholder, F., Brandemuehl, M., Price, H., Netter, J., Kutscher, C., Wolfrum, E., 2007. Parabolic trough receiver thermal testing. In: Energy Sustainability, ASME 2007 Energy Sustainability Conference. pp. 961–970.

Camacho, E., Gallego, A., 2013. Optimal operation in solar trough plants: A case study. Solar Energy 95, 106 – 117.

Camacho, E. F., Berenguel, M., Rubio, F. R., 1997. Advanced Control of Solar Plants. Springer Science & Business Media.

Camacho, E. F., Bordons, C., 2007. Model Predictive control, 2nd Edition. Springer-Verlag London.

Camacho, E. F., Rubio, F. R., Berenguel, M., Valenzuela, L., 2007. A survey on control schemes for distributed solar collector fields. part i: Modeling and basic control approaches. Solar Energy 81 (10), 1240 – 1251.

Camacho, E. F., Soria, M. B., Rubio, F. R., Martínez, D., 2012. Control of Solar Energy Systems, 1st Edition. Springer-Verlag London.

Carmona, R., 1985. Analisis, modelado y control de un campo de colectores solares distribuidos con sistema de seguimiento en un eje. Ph.D. thesis. Universidad de Sevilla.

Cojocaru, E. G., Bravo, J. M., Vasallo, M. J., Santos, D. M., 2019. Optimal scheduling in concentrating solar power plants oriented to low generation cycling. Renewable Energy 135, 789 – 799.

Gallego, A. J., Macías, M., de Castilla, F., Camacho, E. F., 2019. Mathematical modeling of the mojave solar plants. Energies 12 (21).

Gallego, A. J., Yebra, L., Camacho, E. F., Sánchez, A. J., 09 2016. Mathematical modeling of the parabolic trough collector field of the tcp-100 research plant. In: Conference: Modelling and Simulation - 9th EUROSIM 2016, At Oulu, Finland. pp. 912–918.

Geyer, M., Lüpfert, E., Osuna, R., Esteban, A., Schiel, W., Schweitzer, A., Zarza, E., Nava, P., Langenkamp, J., Mandelberg, E., Sep. 2002. Eurotrough - parabolic trough collector developed for cost efficient solar power generation. In: 11th SolarPACES International Symposium on Concentrated Solar Power and Chemical Energy Technologies.

González-Roubaud, E., Pérez-Osorio, D., Prieto, C., 2017. Review of commercial thermal energy storage in concentrated solar power plants: Steam vs. molten salts. Renewable and Sustainable Energy Reviews 80, 133 – 148.

Goswami, D., Kreith, F., Kreider, J., 2000. Principles of Solar Engineering., 2nd Edition. Taylor & Francis.

Helioscsp.com News, May 2020. Abengoa dubai concentrated solar power contract valued at $650mn. http://helioscsp.com/abengoa-dubai-concentrated-solar-power-contract-valued-at-650mn/.

Heney, P. J., May 2020. Positioning parabolic troughs. helac corp. skyfuel inc.
URL `https://www.helac.com/uploads/file/success-stories/Energy/DW_OnSun_Success_Story.pdf`

Kearney, D. W., 2007. Parabolic trough collector overview. Parabolic trough work-shop, NREL.

Khoukhi, B., Tadjine, M., Boucherit, M. S., May 2015. Nonlinear continuous-time generalized predictive control of solar power plant. Int. J. Simul. Multisci. Des. Optim. 6.

Lima, D. M., Normey-Rico, J. E., Santos, T. L. M., 2016. Temperature control in a solar collector field using filtered dynamic matrix control. ISA Transactions 62, 39 – 49, sI: Control of Renewable Energy Systems.

Liu, M., Tay, N. S., Bell, S., Belusko, M., Jacob, R., Will, G., Saman, W., Bruno, F., 2016. Review on concentrating solar power plants and new developments in high temperature thermal energy storage technologies. Renewable and Sustainable Energy Reviews 53, 1411

– 1432.

Lüpfert, E., Riffelmann, K., Price, H., Burkholder, F., Moss, T., May 2008. Experimental analysis of overall thermal properties of parabolic trough receivers. Journal of Solar Energy Engineering 130 (2).

Montañés, R. M., Windahl, J., Palsson, J., Thern, M., 2018. Dynamic modeling of a parabolic trough solar thermal power plant with thermal storage using modelica. Heat Transfer Engineering 39 (3), 277–292.

NREL DEWA, May 2020. Concentrating Solar Power Projects. DEWA CSP Trough Project.
URL https://solarpaces.nrel.gov/dewa-csp-trough-project

NREL Extresol, May 2020. Concentrated Solar Power Projects. Extesol-1.
URL https://solarpaces.nrel.gov/extresol-1

NREL Guzmán, May 2020. Concentrated Solar Power Projects. Guzmán.
URL https://solarpaces.nrel.gov/guzman

NREL Helios, May 2020. Concentrated Solar Power Projects. Helios I.
URL https://solarpaces.nrel.gov/helios-i

NREL KAXU, May 2020. Concentrated Solar Power Projects. Kaxu Solar One.
URL https://solarpaces.nrel.gov/kaxu-solar-one

NREL Majadas, May 2020. Concentrating Solar Power Projects. Majadas I.
URL https://solarpaces.nrel.gov/majadas-i

NREL Solaben, May 2020. Concentrated Solar Power Projects. Solaben 2.
URL https://solarpaces.nrel.gov/solaben-2

NREL Solana, May 2020. Concentrated Solar Power Projects. Solana Generating Station.
URL https://solarpaces.nrel.gov/solana-generating-station

Peiró, G., Prieto, C., Gasia, J., Jové, A., Miró, L., Cabeza, L. F., 2018. Two-tank molten salts thermal energy storage system for solar power plants at pilot plant scale: Lessons learnt and recommendations for its design, start-up and operation. Renewable Energy 121, 236 – 248.

Pelay, U., Luo, L., Fan, Y., Stitou, D., Rood, M., 2017. Thermal energy storage systems for concentrated solar power plants. Renewable and Sustainable Energy Reviews 79, 82 – 100.

Pitz-Paal, R., 2018. Concept and status of concentrating solar power systems. EPJ Web Conf. 189.

Prieto, C., Rodríguez, A., Patiño, D., Cabeza, L. F., 2018. Thermal energy storage evaluation in direct steam generation solar plants. Solar Energy 159, 501 – 509.

Roca, L., Bonilla, J., Rodríguez-García, M. M., Palenzuela, P., de la Calle, A., Valenzuela, L., 2016. Control strategies in a thermal oil – molten salt heat exchanger. AIP Conference Proceedings 1734 (1), 130017.

Romero, M., González-Aguilar, J., 2014. Solar thermal csp technology. Wiley Interdisciplinary Reviews: Energy and Environment 3 (1), 42–59.

Sánchez, A. J., Gallego, A. J., Escaño, J. M., Camacho, E. F., Nov. 2018. Event-based mpc for defocusing and power production of a parabolic trough plant under power limitation. Solar Energy 174, 570 – 581.

Sánchez, A. J., Gallego, A. J., Escaño, J. M., Camacho, E. F., May 2019a. Adaptive incremental state space mpc for collector defocusing of a parabolic trough plant. Solar Energy 184, 105–114.

Sánchez, A. J., Gallego, A. J., Escaño, J. M., Camacho, E. F., Sep. 2019b. Thermal balance of large scale parabolic trough plants: A case study. Solar Energy 190, 69 – 81.

Sarbu, I., Sebarchievici, C., Jan. 2018. A comprehensive review of thermal energy storage. Sustainability 10 (1), 1–32.

Schenk, H., Dersch, J., Hirsch, T., Polklas, T., Sep. 2015. Transient simulation of the power block in a parabolic trough power plant. In: The 11th International Modelica Conference Versailles, France. Linköping University Electronic Press, Linköpings universitet, pp. 605–614.

SCHOTT Solar CSP GmbH, May 2020. Schott ptr®70 receivers.
URL https://www.us.schott.com/csp/english/schott-solar-ptr-70-receivers.html

System Advisor Model (SAM). NREL, Sep. 2018.
URL https://sam.nrel.gov/

Therminol VP1 HTF, May 2020.
URL https://www.therminol.com/products/Therminol-VP1

Vasallo, M. J., Bravo, J. M., 2016. A mpc approach for optimal generation scheduling in csp plants. Applied Energy 165, 357 – 370.